Causes and Probability of Occurrence of Extreme Precipitation Events like Chennai 2015

LAKSHMI KRISHNAMURTHY,[a,b] GABRIEL A. VECCHI,[c,d] XIAOSONG YANG,[a,e] KARIN VAN DER WIEL,[f] V. BALAJI,[a,g] SARAH B. KAPNICK,[a] LIWEI JIA,[h,i] FANRONG ZENG,[a] KAREN PAFFENDORF,[a,b] AND SETH UNDERWOOD[a]

[a] *NOAA/Geophysical Fluid Dynamics Laboratory, Princeton, New Jersey*
[b] *Atmospheric and Oceanic Sciences Program, Princeton University, Princeton, New Jersey*
[c] *Department of Geosciences, Princeton University, Princeton, New Jersey*
[d] *Princeton Environmental Institute, Princeton University, Princeton, New Jersey*
[e] *University Corporation for Atmospheric Research, Boulder, Colorado*
[f] *Royal Netherlands Meteorological Institute, De Bilt, Netherlands*
[g] *Cooperative Institute for Climate Science, Princeton University, Princeton, New Jersey*
[h] *NOAA/NWS/NCEP/Climate Prediction Center, College Park, Maryland*
[i] *Innovim, LLC, Greenbelt, Maryland*

(Manuscript received 8 May 2017, in final form 26 January 2018)

ABSTRACT

Unprecedented high-intensity flooding induced by extreme precipitation was reported over Chennai in India during November–December of 2015, which led to extensive damage to human life and property. It is of utmost importance to determine the odds of occurrence of such extreme floods in the future, and the related climate phenomena, for planning and mitigation purposes. Here, a suite of simulations from GFDL high-resolution coupled climate models are used to investigate the odds of occurrence of extreme floods induced by extreme precipitation over Chennai and the role of radiative forcing and/or large-scale SST forcing in enhancing the probability of such events in the future. The climate of twentieth-century experiments with large ensembles suggest that the radiative forcing may not enhance the probability of extreme floods over Chennai. Doubling of CO_2 experiments also fails to show evidence for an increase of such events in a global warming scenario. Further, this study explores the role of SST forcing from the Indian and Pacific Oceans on the odds of occurrence of Chennai-like floods. Neither El Niño nor La Niña enhances the probability of extreme floods over Chennai. However, a warm Bay of Bengal tends to increase the odds of occurrence of extreme Chennai-like floods. In order to trigger a Chennai like-flood, a conducive weather event, such as a tropical depression over the Bay of Bengal with strong transport of moisture from a moist atmosphere over the warm Bay, is necessary for the intense precipitation.

1. Introduction

The city of Chennai in India experienced a catastrophic flooding event in November–December of 2015. During these months, Chennai received 1416.8 mm of rainfall, more than 3 times the rainfall climatology of 408.4 mm (Ray et al. 2016). It led to flooding in large areas and displaced more than 1.8 million people (Selvaraj et al. 2016; Narasimhan et al. 2016). This event caused widespread destruction of life and property, affecting 4 million people and leading to a monetary loss of 3 billion U.S. dollars (Narasimhan et al. 2016; Mishra 2016; Ray et al. 2016). It was estimated to be the eighth most expensive natural disaster in the world during 2015 (DNA 2015). Therefore, it is important to understand the probability of occurrence of such an event in the future and its causes, for planning and mitigation purposes.

Unlike most of India, Chennai receives rainfall as part of the northeast monsoon during the October–December months. The northeast monsoon rainfall (also referred to as winter monsoon) contributes 50% of the annual rainfall over the southeastern coast of the Indian Peninsula, significantly affecting the water resources and agricultural production in the region (Kumar et al. 2007). The northeast monsoon is associated with dry northeasterly winds from the Himalayas and Indo-Gangetic Plain regaining moisture from the

Corresponding author: Lakshmi Krishnamurthy, lakshmi.krishnamurthy@noaa.gov

DOI: 10.1175/JCLI-D-17-0302.1

Bay of Bengal, resulting in heavy rainfall over the southern peninsular region.

The total northeast monsoon rainfall (though not counting extreme events) is significantly correlated with El Niño–Southern Oscillation (ENSO; Nayagam et al. 2009; Kumar et al. 2007; Yadav 2012), and the relationship has strengthened in recent decades (Kumar et al. 2007; Zubair and Ropelewski 2006). This may be attributed to the enhanced relationship between ENSO and Bay of Bengal sea surface temperatures (SSTs) after the 1970s, stronger easterly anomalies and associated moisture convergence that are favorable for the northeast monsoon rainfall (Kumar et al. 2007), and intensified convection due to warmer Indian Ocean SSTs and the strengthening of the circulation associated with El Niño (Zubair and Ropelewski 2006). Yadav (2013) has also highlighted the role of Bay of Bengal SSTs in driving the interannual variability of the northeast monsoon rainfall. The years with warm Bay of Bengal SSTs along with a cold east equatorial Indian Ocean shift the ITCZ northward, and the depressions formed in the north Indian Ocean strike the southern peninsula, leading to enhanced northeast monsoon rainfall. In addition, the northeast monsoon rainfall is shown to be associated with above-normal SSTs in the Arabian Sea and Bay of Bengal (Kumar et al. 2007). The northeast monsoon rainfall is also suggested to increase in response to global warming (Naidu et al. 2012).

Thus, several studies have shown that ENSO, Indian Ocean SSTs, and global warming may lead to enhanced rainfall during the northeast monsoon. Hence, we investigate whether the probability of occurrence of precipitation-induced extreme flood events (such as that experienced in Chennai during November–December of 2015) will increase in the future either because of radiative forcing, large-scale SST forcing such as ENSO, and/or warming in the Indian Ocean or Bay of Bengal. Considering that it is difficult to reliably determine the effects of climate on such a rare extreme event using limited sample size in observations, we make use of a suite of Geophysical Fluid Dynamics Laboratory (GFDL) coupled simulations to investigate the probability of occurrence of extreme precipitation as measured by the 2015 precipitation-induced extreme flooding event in Chennai. Hereafter, while we state ''extreme flood event,'' we are referring to the precipitation extreme that led to flooding, or a ''precipitation-induced extreme flood.'' We carefully make this distinction, as this paper focuses on the atmospheric component of flooding without regard for land surface conditions or the built environment (water management). Data and the models used are described in section 2. Results from this study are presented in section 3, and conclusions are in section 4.

2. Data and models

a. Observations

The SST data on a 1° × 1° spatial grid is derived from the HADISST, version 1.1, from the Met Office Hadley Centre for Climate Change (Rayner et al. 2003) for the period 1870–2016. We make use of a high-resolution observational precipitation dataset, APHRODITE (Yatagai et al. 2012), to evaluate the ability of the models to capture observed rainfall and its teleconnections. APHRODITE rainfall data is created from rain gauge observations and has been interpolated on a 0.25° × 0.25° grid spanning from 1951 to 2007. In addition, the GPCP rainfall dataset is used, which is on a 2.5° × 2.5° resolution for the period 1979–2014 [Adler et al. 2003; GPCP data provided by the NOAA/OAR/ESRL Physical Sciences Division (PSD), Boulder, Colorado, from their website at http://www.esrl.noaa.gov/psd/]. GPCP data is based on data from rain gauge stations, satellites, and sounding observations that have been merged to estimate monthly rainfall. We also use satellite-based daily rainfall data from the Tropical Rainfall Measuring Mission (TRMM; Simpson et al. 1996) for November–December of 2015, which is on a high-resolution grid of 0.25° × 0.25°. Another high-resolution gridded precipitation dataset from the University of Delaware is used, which is on 0.5° longitude × 0.5° latitude for the period 1900–2010 (Legates and Willmott 1990). Daily SLP for November–December of 2015 is from a global atmospheric reanalysis product, ERA-Interim (Dee et al. 2011), produced by the European Centre for Medium-Range Weather Forecasts (ECMWF). SLP data is on a 0.75° × 0.75° spatial grid.

b. Models

We use a suite of GFDL models for our investigation: Climate Model, version 2.1 (CM2.1; Delworth et al. 2012), the Forecast-Oriented Low Ocean Resolution model (FLOR; Vecchi et al. 2014), the flux-adjusted version of FLOR (FLOR-FA; Vecchi et al. 2014), and a high-resolution version of FLOR (HiFLOR; Murakami et al. 2015a). FLOR comprises high-resolution atmosphere and land components (0.5° × 0.5°) and a low-resolution ocean component at 1°. FLOR-FA is the flux-adjusted version of FLOR, which has been artificially bias-corrected to provide climatological SST and wind stress close to observed estimates. FLOR and FLOR-FA are known to have better climate simulation

than CM2.1, which further leads to improved simulation of teleconnections and predictions (Vecchi et al. 2014; Msadek et al. 2014; Winton et al. 2014; Jia et al. 2015; Yang et al. 2015; Krishnamurthy et al. 2015; Delworth and Zeng 2016; Zhang and Delworth 2015; Krishnamurthy et al. 2016). The high-resolution version of FLOR, HiFLOR, has a resolution of atmosphere and land at 25 km and the same ocean resolution as FLOR. HiFLOR improves the simulation and prediction of frequency and intensity of tropical cyclones (TCs) compared to FLOR (Murakami et al. 2015a), and better reproduces precipitation extremes over the United States (van der Wiel et al. 2016) and surge events over the Gulf of California (Pascale et al. 2016).

We use preindustrial (1860-control), present-day (1990-control), climate of the twentieth century (20C3M), and $2xCO_2$ simulations from CM2.1, FLOR, FLOR-FA, and HiFLOR to evaluate the model in simulating the northeast monsoon and teleconnections, and investigate if the probability of extreme flood events over Chennai increases in the future . Preindustrial and present-day control simulations have radiative forcing fixed at 1860 and 1990 levels, respectively. The number of years of data used for our analysis is 200, 600, 500, and 300 for present-day control simulations using CM2.1, FLOR, FLOR-FA, and HiFLOR, which will be referred to hereafter as CM2.1-1990, FLOR-1990, FLOR-FA-1990, and HiFLOR-1990, respectively. To test the ability of GFDL models to simulate the mean monsoon and its teleconnections, we predominantly use the 1990 control runs, unless otherwise noted. For preindustrial control simulations, we make use of 900, 900, and 2000 years of data from CM2.1, FLOR, and FLOR-FA, which will be referred to hereafter as CM2.1-1860, FLOR-1860, and FLOR-FA-1860, respectively.

In addition, in order to understand the future changes in the probability of Chennai-like flood events, historical forcing simulations are also utilized from FLOR and FLOR-FA, which will be referred to as FLOR-20C3M and FLOR-FA-20C3M, respectively. Both FLOR and FLOR-FA have 5-member ensembles integrated from 1861 to 2040, where historical anthropogenic and aerosol forcing are prescribed from 1861 to 2005 and an RCP4.5 scenario is prescribed from 2006 onward with no volcanic forcing beyond 2006. A 35-member ensemble of FLOR-FA is also used, which is integrated from 1941 to 2040 with a similar forcing scenario as the above 5-member ensemble. This large ensemble data from FLOR and FLOR-FA has been successfully used in attribution studies of hurricanes over Hawaii (Murakami et al. 2015b), accumulated cyclone energy over the west North Pacific Ocean (Zhang et al. 2016), winter storms (Yang et al. 2015), heat waves (Jia et al. 2016), and precipitation-induced extreme floods (van der Wiel et al. 2017) over the United States.

To explore the effect of increasing greenhouse gases on extreme flood events, we also analyze the $2xCO_2$ runs based on the FLOR-FA-1990 simulation, which will be referred to as FLOR-FA-1990.2CO2. It comprises a 2-member ensemble, which starts at year 101 of the FLOR-FA-1990 run with CO_2 increasing at the rate of 1% yr^{-1}, doubling after 70 yr and held constant thereafter. We use 210 yr of data for our analysis. This model run has also been used in the study of precipitation extremes over the United States (van der Wiel et al. 2016, 2017).

3. Results

a. *Simulation of the northeast monsoon*

1) Mean state and variability

We first investigate the ability of the suite of GFDL models to simulate the mean state and variability of the northeast monsoon rainfall. Since we are motivated to understand the probability of occurrence of Chennai-like flood events in the future, we show the results for November–December, which coincide with the peak rainfall over Chennai during 2015. The CM2.1 model simulates weaker-than-observed mean rainfall over the northeast monsoon region (Figs. 1a,c). The higher-resolution FLOR model improves the simulation of mean rainfall (Fig. 1e). FLOR-FA, the flux-adjusted version of FLOR, shows further improvement in simulation of mean rainfall (Fig. 1g), especially over coastal regions, although the mean is slightly higher than in observations. Similarly, FLOR and FLOR-FA have a more realistic representation of observed variability of the northeast monsoon rainfall compared to CM2.1 (Figs. 1b,d,f,h).

2) Relation to large-scale climate: ENSO and Bay of Bengal SSTs

The northeast monsoon rainfall is significantly correlated with ENSO (Nayagam et al. 2009; Kumar et al. 2007; Zubair and Ropelewski 2006). Considering that a strong El Niño event in the tropical Pacific (Chen et al. 2016) coincided with the extreme Chennai flood event of 2015, it is important to understand if ENSO might increase the probability of occurrence of such an extreme event. Before we investigate the effect of ENSO on extreme floods, we first explore the ability of the GFDL models to simulate the relationship between ENSO and the northeast monsoon rainfall during November–December. We define a rainfall index over the domain

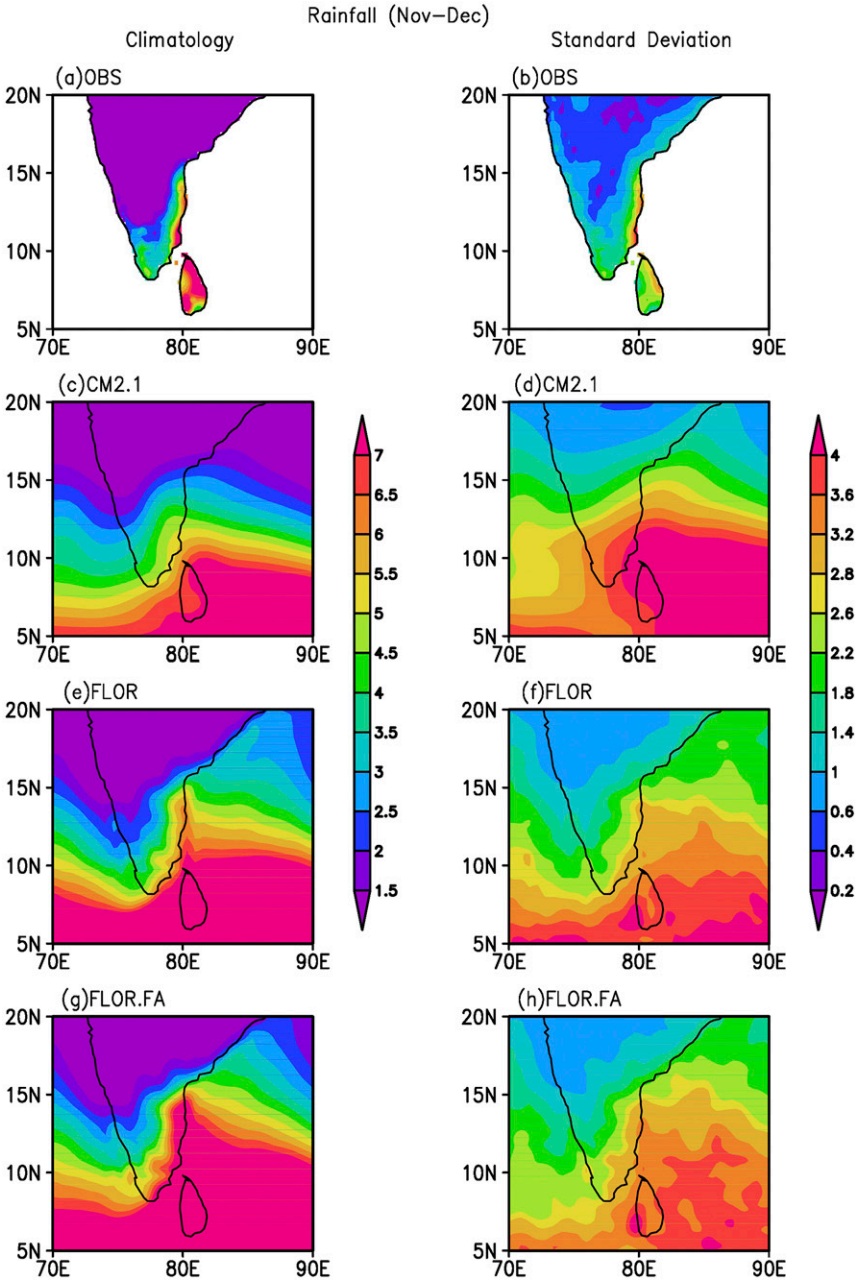

FIG. 1. Climatology of rainfall for (a) observations, (c) CM2.1-1990, (e) FLOR-1990, and (g) FLOR-FA-1990, and std dev of rainfall for (b) observations, (d) CM2.1-1990, (f) FLOR-1990, and (h) FLOR-FA-1990 during November–December. Units of rainfall are in mm day^{-1}.

[8°–17°N, 70°–82°E] as a representative of the northeast Indian monsoon rainfall (herein referred to as the NE-IMR index.)[1] Regression of rainfall and SST on NE-IMR based on observations suggests that the enhanced northeast monsoon rainfall is associated with El Niño in the tropical Pacific and above-normal SSTs in the Bay of Bengal (Figs. 2a,b). However, CM2.1 shows the opposite relationship between ENSO and the northeast monsoon rainfall, with enhanced rainfall associated with La Niña in contrast to observations (Figs. 2c,d). The northeast monsoon rainfall has no systematic multicentennial relation with the tropical Pacific SSTs in FLOR and FLOR-FA (Figs. 2e–h). We also show the long-term

[1] Index is defined over land for observations and includes data over both land and ocean for model. Analysis is repeated using only land points for model and the results were robust.

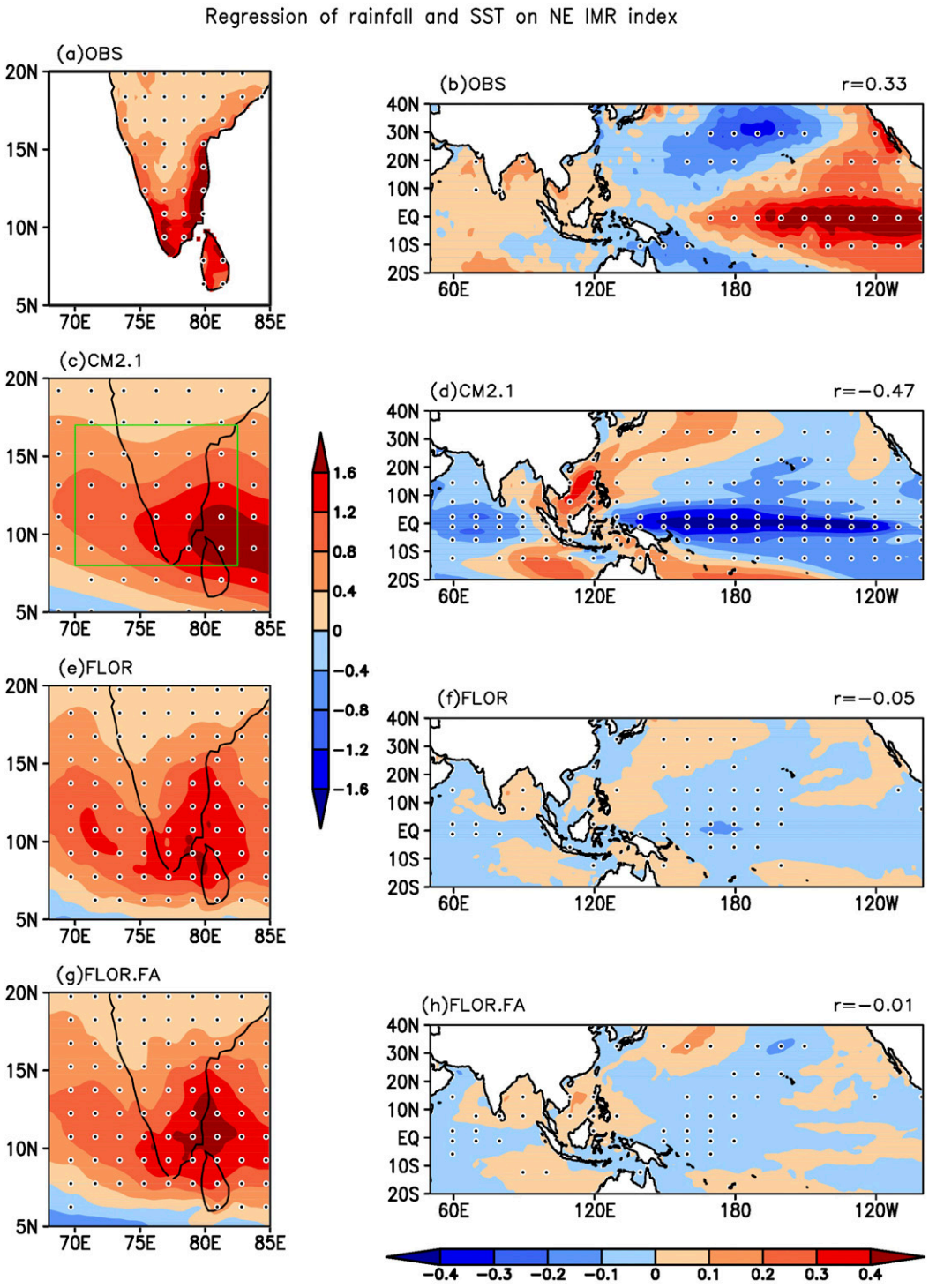

FIG. 2. Regression of November –December rainfall on November –December NE-IMR index for (a) observations, (c) CM2.1-1990, (e) FLOR-1990, and (g) FLOR-FA-1990. Units are in millimeters per day per std dev of the corresponding time series. Regression of November –December SST on November –December NE-IMR index for (b) observations, (d) CM2.1-1990, (f) FLOR-1990, and (h) FLOR-FA-1990. Units are in °C per std dev of corresponding time series. Dotted regions represent values significant at 5% significance level. Green box in (c) represents the area over which the NE-IMR index is constructed. Correlation between the Niño-3.4 and the NE-IMR is shown on top right side of (b), (d), (f), and (h).

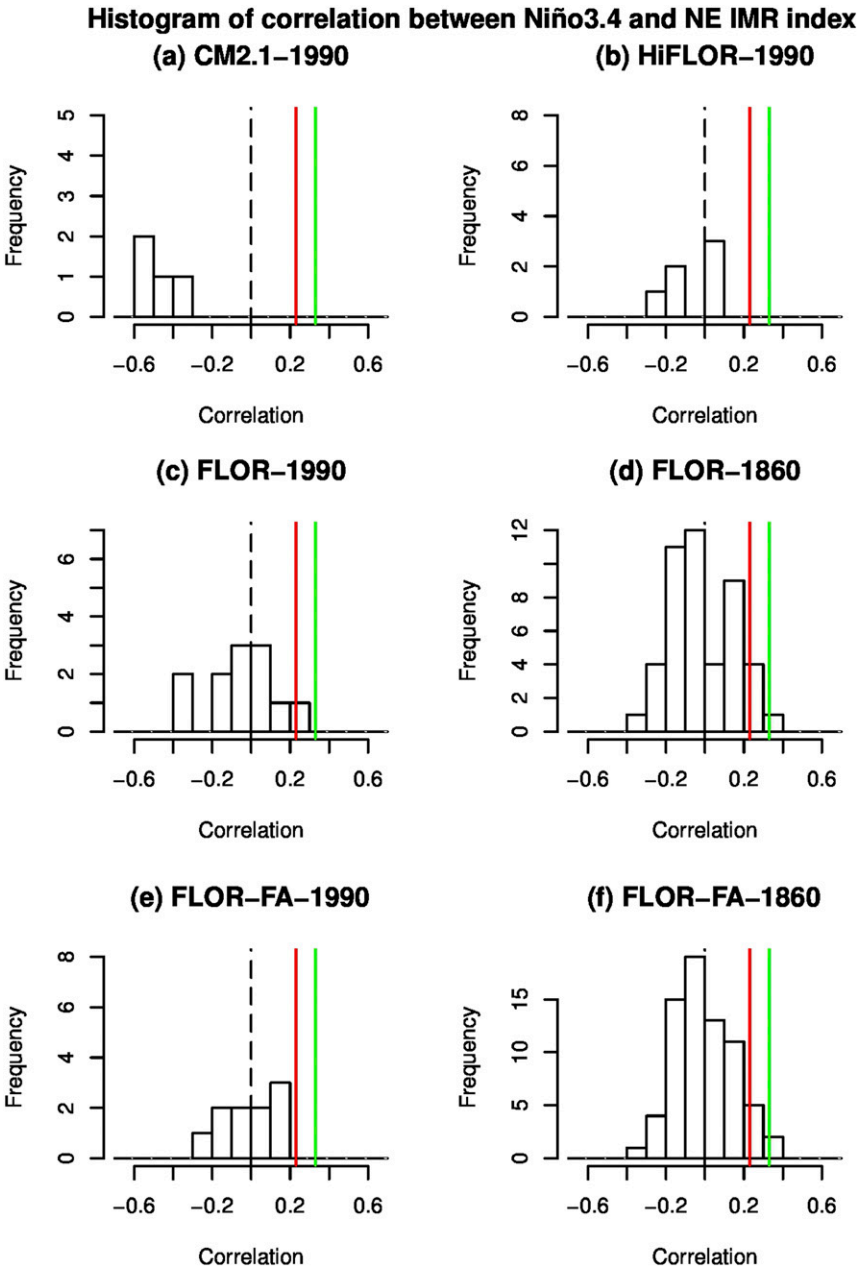

FIG. 3. Histogram of correlations between Niño-3.4 and NE-IMR indices for 50-yr time slices during November –December for (a) CM2.1-1990, (b) HiFLOR-1990, (c) FLOR-1990, (d) FLOR-1860, (e) FLOR-FA-1990, and (f) FLOR-FA-1860. The red and green vertical lines refer to correlation values based on obs data for GPCP and APHRODITE, respectively. Black vertical bars correspond to model. Correlation values greater than 0.27, 0.22, and 0.23 are significant at 5% level for GPCP, APHRODITE, and models, respectively.

correlation between Niño-3.4 and NE-IMR (noted in top corner of Figs. 2b,d,f,h). The long-term relationship between ENSO and the northeast monsoon is negative in CM2.1 compared to positive in observations, and is close to zero in FLOR and FLOR-FA. We need to understand if this negative or weak relationship in GFDL models is related to either the model's inability to capture the observed relation or related to sampling variability, as we note that these model results are based on 200 years of CM2.1, 600 years of FLOR, and 500 years of FLOR-FA, whereas the observational analysis is based on 57 years.

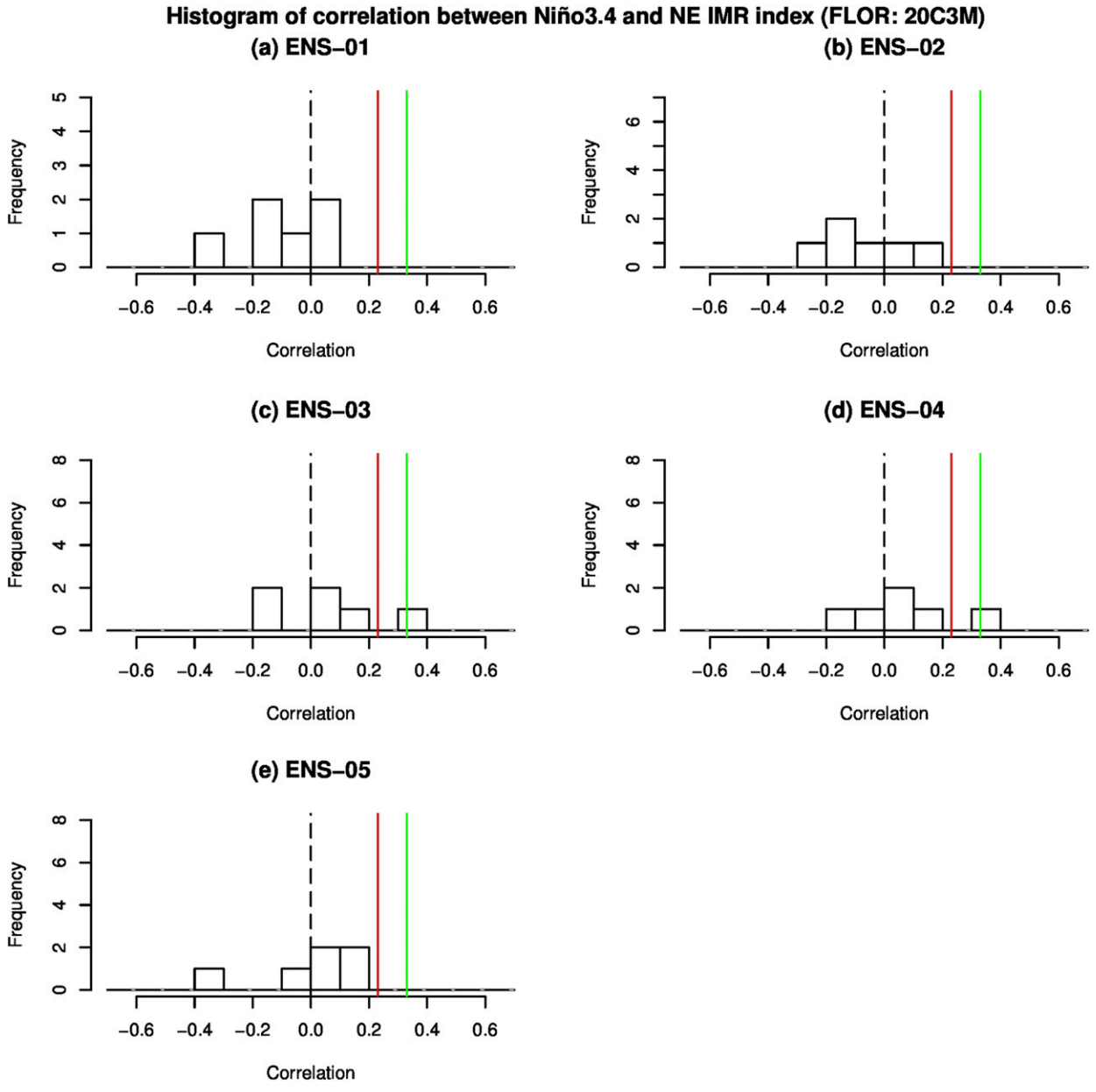

FIG. 4. Histogram of correlations between Niño-3.4 and NE-IMR indices for 40-yr time slices during November –December in FLOR-20C3M for (a) ensemble member 1, (b) ensemble member 2, (c) ensemble member 3, (d) ensemble member 4, and (e) ensemble member 5. The red and green vertical lines refer to correlation values based on obs data for GPCP and APHRODITE, respectively. Black vertical bars correspond to model. Correlation values greater than 0.27, 0.22, and 0.26 are significant at 5% level for GPCP, APHRODITE, and model, respectively.

Thus, in order to determine if the lack of ability of GFDL models to simulate the apparent observed relationship is due to sampling variability, the correlations are calculated for every 40- or 50-yr time slices (considering a sample size similar to observations). For this purpose, we make use of long control simulations of CM2.1 and several versions of FLOR runs such as the preindustrial control run and present-day control run from FLOR, the flux-adjusted version of FLOR and the high-resolution version of FLOR, and the climate of twentieth-century ensemble runs from FLOR and FLOR-FA (only figures for FLOR-20C3M are shown; FLOR-FA-20C3M shows similar results). The model suite produces correlation values ranging from −0.6 to 0.4 (Figs. 3 and 4). CM2.1 shows predominantly negative correlation values between Niño-3.4 and NE-IMR and

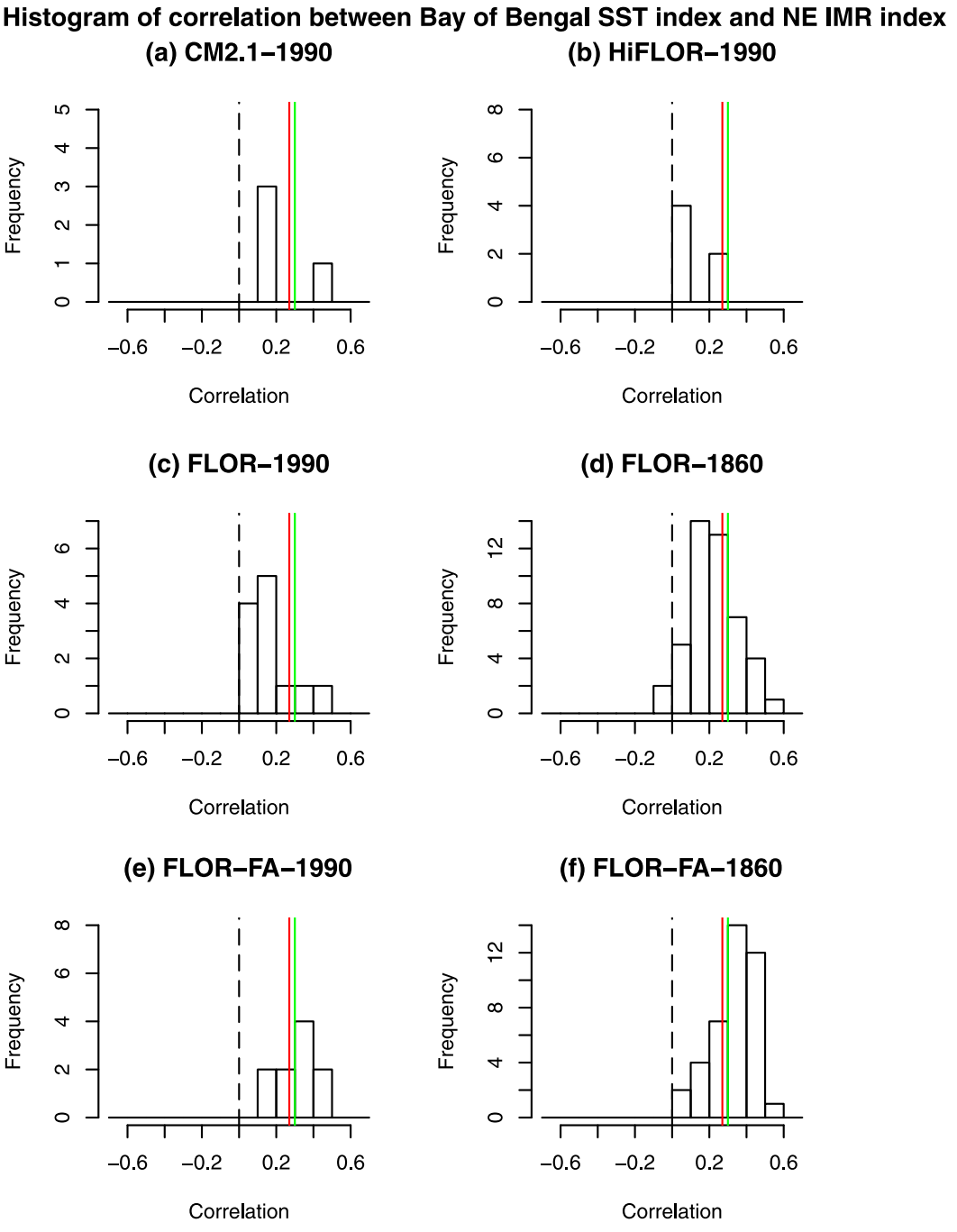

FIG. 5. Histogram of correlations between the Bay of Bengal SST index and NE-IMR index for 50-yr time slices during November–December for (a) CM2.1-1990, (b) HiFLOR-1990, (c) FLOR-1990, (d) FLOR-1860, (e) FLOR-FA-1990, and (f) FLOR-FA-1860. The red and green vertical lines refer to correlation values based on obs data for GPCP and APHRODITE, respectively. Black vertical bars correspond to model. Correlation values greater than 0.27, 0.22, and 0.23 are significant at 5% level for GPCP, APHRODITE, and models, respectively.

thus fails to capture the observed correlation (Fig. 3a). Correlation analysis with the CM2.1-1860 control run also yields a similar result (figure not shown). HiFLOR shows values ranging from −0.3 to 0.1 and therefore lacks in its ability in simulating the observed relationship (Fig. 3b). The correlation values in FLOR and FLOR-FA simulations range from −0.4 to +0.4 (Figs. 3c,d,e,f). Hence, in FLOR and FLOR-FA, there are some time

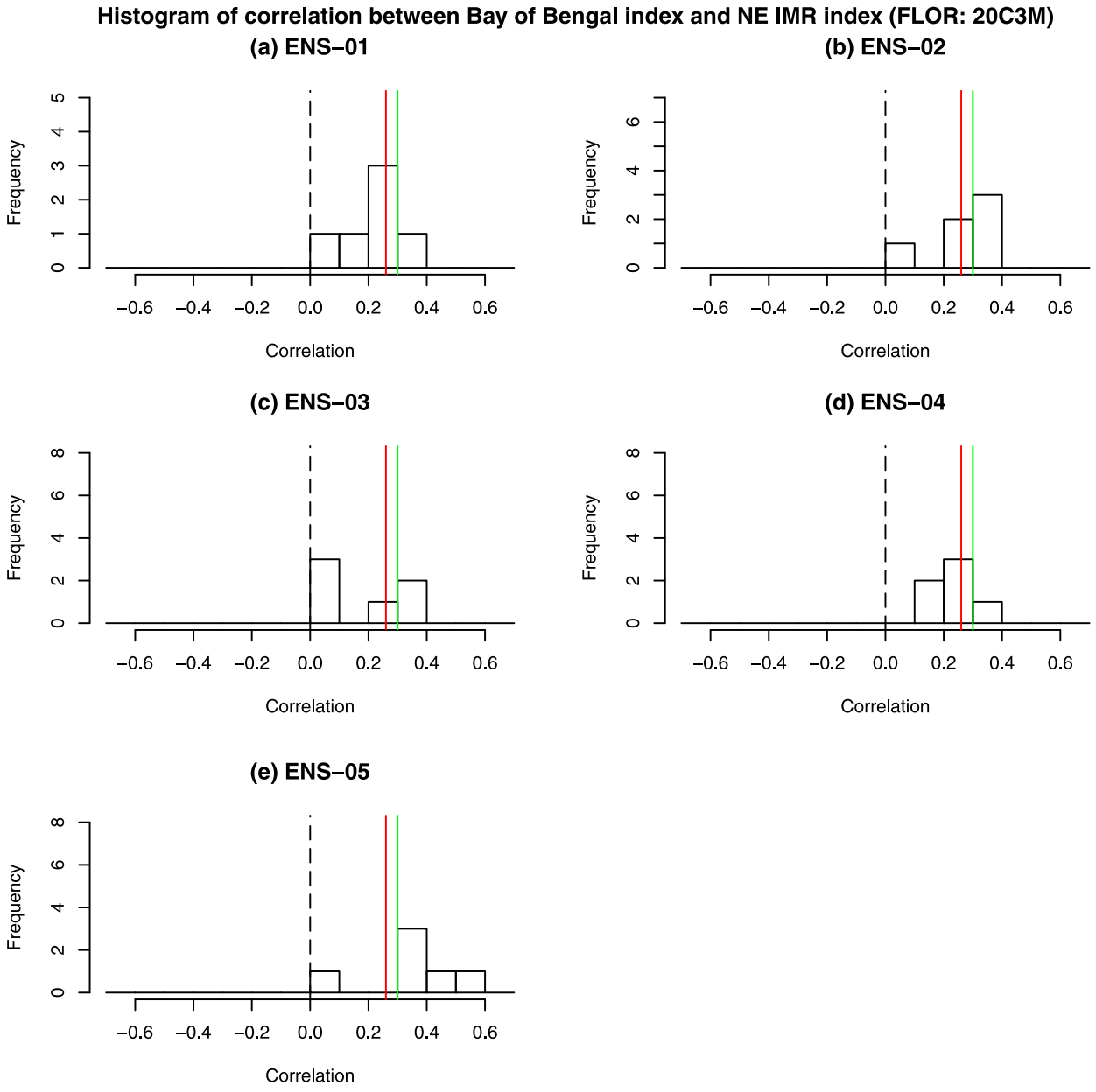

FIG. 6. Histogram of correlations between the Bay of Bengal SST index and NE-IMR index for 40-yr time slices during November –December in FLOR-20C3M for (a) ensemble member 1, (b) ensemble member 2, (c) ensemble member 3, (d) ensemble member 4, and (e) ensemble member 5. The red and green vertical lines refer to correlation values based on obs data for GPCP and APHRODITE, respectively. Black vertical bars correspond to model. Correlation values greater than 0.27, 0.22, and 0.26 are significant at 5% level for GPCP, APHRODITE, and model, respectively.

slices in which the correlation value is close to observations, that is, 0.3, and the wide spectrum of correlation values in the models falls within the range of the observed correlation between ENSO and the northeast monsoon rainfall. This is within the range of variability of ENSO–monsoon relation in observations. Rajeevan et al. (2012) and Yadav (2013) show that the ENSO–monsoon relationship undergoes decadal variations with correlations spanning from approximately −0.2 to 0.4. Yadav (2013) has also suggested the significant role of the Bay of Bengal SSTs on the northeast monsoon. Thus, we perform a similar analysis as in Figs. 3 and 4 for the relationship between the Bay of Bengal SSTs and the northeast monsoon rainfall (Figs. 5 and 6). Although CM2.1-1990 does not capture the observed relationship between the northeast monsoon and Bay of Bengal SSTs

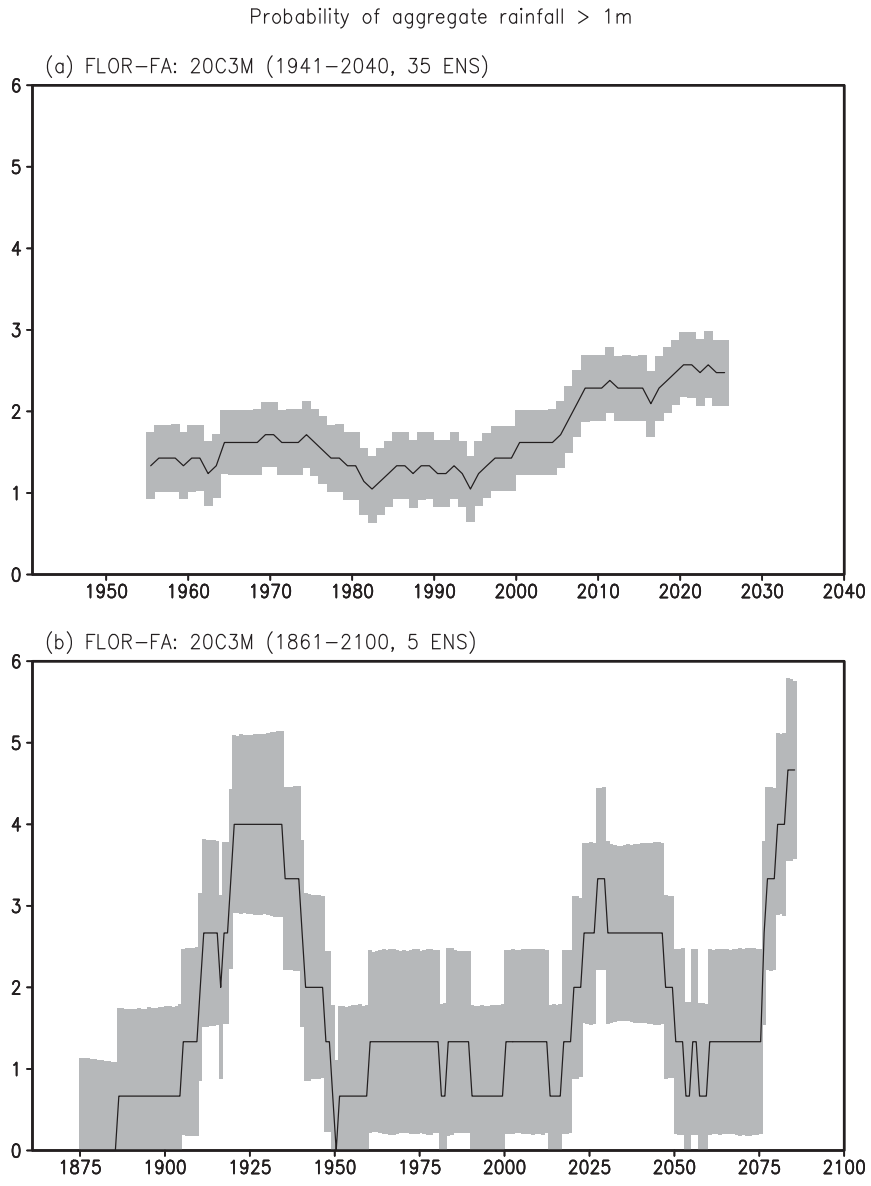

FIG. 7. Probability of aggregate rainfall greater than 1 m in FLOR-FA-20C3M based on (a) 35 ensemble members for 1941–2040 and (b) 5 ensemble members for 1861–2100 in a 30-yr moving window. Shaded regions represent the std error calculated from a bootstrap sample.

(Fig. 6a), CM2.1-1860 does simulate this relationship (figure not shown). FLOR models successfully capture the observed range of correlation between the Bay of Bengal SST and northeast monsoon rainfall. We have also explored the probability distribution function of rainfall anomalies at Chennai during El Niño and La Niña years using the model simulations and gridded rainfall data from the University of Delaware, and they suggest similar conclusions as the correlation analysis (figures not shown). Therefore, we conclude that the FLOR and FLOR-FA models capture the variations in the observed SST–monsoon relation and are suitable to investigate if the probability of the extreme northeast monsoon rainfall events increases during ENSO and Bay of Bengal SST events.

b. Role of radiative forcing

Based on the results stated in section 3a(1) and 3a(2), we conclude that the FLOR and FLOR-FA models adequately simulate the mean state, variability, and teleconnections associated with the northeast monsoon. Thus, we make use of FLOR and FLOR-FA to investigate if the radiative forcing increases the odds of occurrence of Chennai-like flood events in the future.

Since we are investigating the Chennai-flood event, hereafter we analyze the rainfall at the grid point over Chennai (13.08°N, 80.27°E). The accumulated rainfall over Chennai was 1416.8 mm during November–December of 2015 (Ray et al. 2016); thus, we use the criteria of 1 m to investigate the probability of occurrence of a Chennai-like flood event and the factors that may lead to such events. Based on the FLOR-FA-1860 run, 1 m of rainfall corresponds to the 97.8th percentile. The probability of aggregate rainfall greater than 1 m in FLOR-FA-20C3M based on 35 ensemble members from 1941 to 2040 shows an increasing trend from 2000 onward (Fig. 7a), suggesting an increase in Chennai-like flood events in the future consistent with the observed increasing trend of the northeast monsoon rainfall (Rajeevan et al. 2012). However, similar analysis of a longer FLOR-FA-20C3M run based on five ensemble members from 1871 to 2100 does not indicate any trend in rainfall (Fig. 7b), and the trend from 2000 onward as seen in Fig. 7a appears to be part of long-term variability. Thus, there is no indication that radiative forcing increases the probability of Chennai-like flood events in future. Similar analysis of long simulations using increased ensemble size will enhance the confidence in these results.

It has been shown in observations that extreme rainfall events during the northeast monsoon increase under global warming (Naidu et al. 2012; Prakash et al. 2013). Thus, we also explore the possibility of an increase in Chennai-like flood events in a warming scenario. We calculate the probability of aggregate rainfall greater than 1 m in the $2xCO_2$ run and compare these probabilities to the preindustrial and present-day control simulations (Fig. 8). Although the 1990-control run shows a higher probability of Chennai-like floods relative to the 1860-control run, the probability of aggregate rainfall greater than 1 m over Chennai is not higher than the 1990-control run when the CO_2 concentration is doubled. Thus, based on Fig. 8, it is inconclusive that the probability of a Chennai-like flood event may increase in a warming scenario. Therefore, we conclude that there is no robust evidence to attribute the Chennai flood event of 2015 to anthropogenic forcing and that there is no evidence either to indicate that the odds of occurrence of Chennai-like flood events may increase in a future warming scenario.

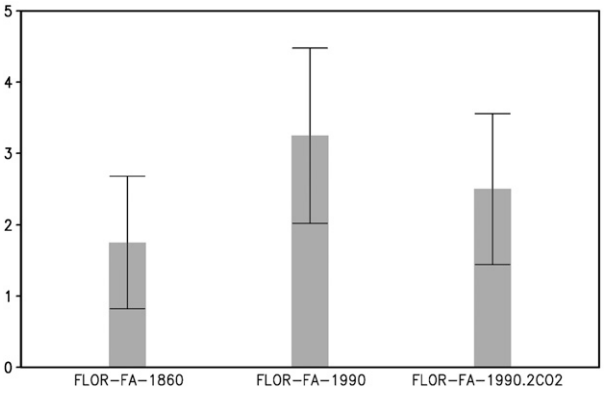

FIG. 8. Probability of aggregate rainfall greater than 1 m in FLOR-FA-1860, FLOR-FA-1990, and FLOR-FA-1990.2CO_2. For FLOR-FA-1860 and FLOR-FA-1990, the sample size is 420 yr each. For FLOR-FA-1990.2CO_2, data is combined from 2 ensemble members of each run for 210 yr, resulting in a total sample size of 420 yr. Vertical lines within shaded bars represent the std error calculated from a bootstrap sample.

c. *Role of large-scale climate: Tropical SSTs*

Further, another group of studies suggests that the observations show an increasing trend of the northeast monsoon rainfall, which is attributed to the increase in the tropical Indo-Pacific SSTs (Yadav 2012; Naidu et al. 2012). Therefore, we explore the effect of large-scale climate such as SSTs in increasing the odds of occurrence of extreme floods over Chennai. Considering that a strong El Niño event was prevalent in the tropical Pacific (L'Heureux et al. 2017) during the extreme Chennai flood event of 2015 and studies suggesting the role of Pacific SSTs in modulating the northeast monsoon (Nayagam et al. 2009; Kumar et al. 2007), we analyzed the conditional probability of rainfall over Chennai during El Niño and La Niña events based on the standardized Niño-3.4 index. Figure 9a suggests that the probability of occurrence of a Chennai-like flood event does not favor either El Niño or La Niña in the tropical Pacific. Thus, the conditional probability of extreme floods during ENSO years suggests that ENSO may not increase the odds of occurrence of extreme flood events over Chennai (Fig. 9a). Further, in order to understand if the SSTs from other oceanic basins might play a role, we construct the composite of SST over those years with aggregate rainfall over Chennai greater than 1 m and compare it to SSTs during 2015 (Fig. 10b). Figure 10b does not show any signature in the tropical Pacific consistent with Fig. 9a. However, comparing the composite to SSTs in 2015, we notice that the warming in the Bay of Bengal is a common signature between Figs. 10a and 10b.

This suggests that the extreme rainfall events may be related to warm Bay of Bengal SSTs. Observational studies have also suggested a link between the northeast monsoon and Indian Ocean SSTs (e.g., Naidu et al. 2012; Yadav 2013). Thus, we construct a Bay of Bengal SST index to understand its effect on Chennai rainfall. The Bay of Bengal SST index is defined as the area-averaged SSTs over the domain [5°–25°N, 80°–100°E]. The SST

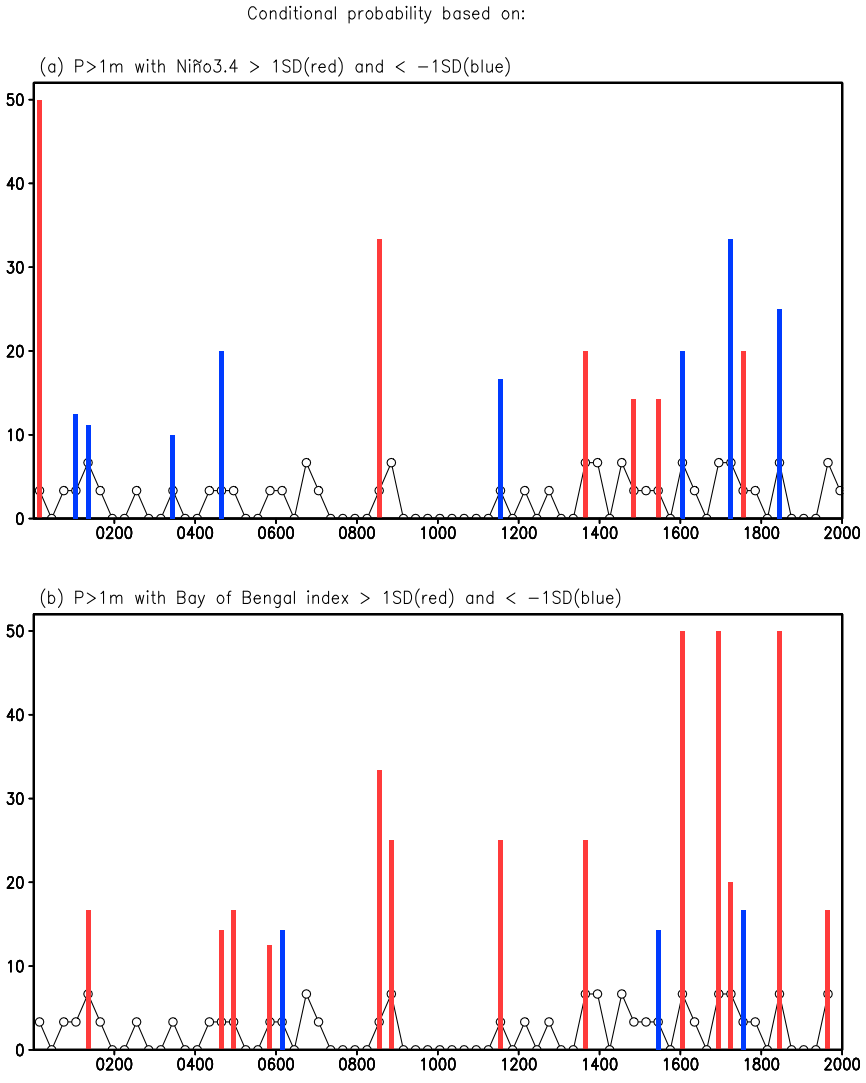

FIG. 9. Conditional probability for November –December based on (a) aggregate rainfall at Chennai greater than 1 m and Niño-3.4 greater than 1.0 SD (red), and aggregate rainfall at Chennai greater than 1 m and Niño-3.4 less than −1.0 SD (blue), and (b) aggregate rainfall at Chennai greater than 1 m and Bay of Bengal SST* index greater than 1.0 SD (red), and aggregate rainfall at Chennai greater than 1 m and Bay of Bengal SST* index less than −1.0 SD (blue). Black solid line with circles represents the probability of aggregate rainfall greater than 1 m over Chennai in both (a) and (b).

index is further detrended to remove any spurious trends and calculated relative to tropical SSTs and hereafter referred to as SST*. We use relative SSTs as precipitation is shown to be sensitive to SST deviations from tropical mean (Vecchi and Soden 2007; Xie et al. 2010). Conditional probability is calculated based on the standardized Bay of Bengal SST* index greater than 1.0 standard deviation (SD) and less than −1.0 SD for rainfall at Chennai greater than 1 m (Fig. 9b). Results suggest that the probability of occurrence of extreme flood events over Chennai is higher when Bay of Bengal SSTs are above normal compared to below normal. We also explore if the probability of an extreme flood event is sensitive to the strength of Bay of Bengal SSTs. Table 1 shows that the warmer the Bay of Bengal SSTs, the higher the probability of occurrence of extreme flood events over Chennai. It is to be noted that these results are based on a single model and with a horizontal resolution of 50 km. These results need to be tested with high-resolution models and with the availability of a longer sample size of observations.

Finally, we investigate the circulation features that are associated with extreme flood events over Chennai. Composites of rainfall for years with aggregate rainfall

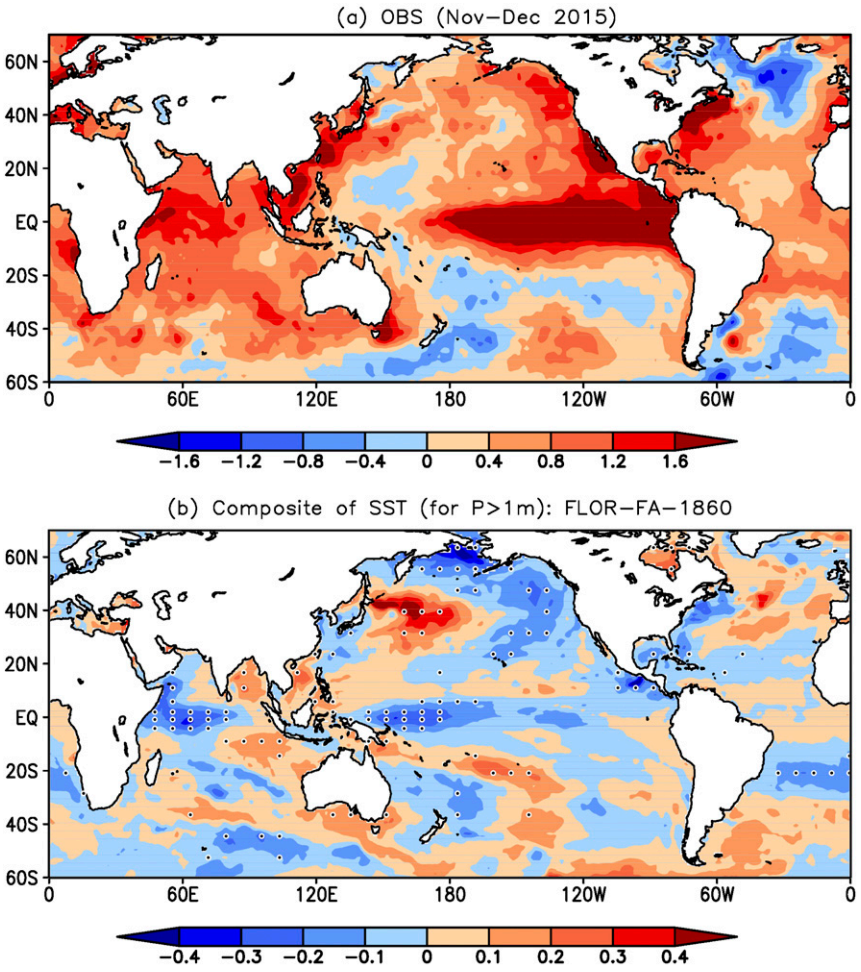

FIG. 10. (a) Obs SST for November –December of 2015 and (b) composite of SST for aggregate rainfall greater than 1 m for FLOR-FA-1860. Units are in °C. Dotted regions represent values significant at 5% significance level.

over Chennai greater than 1 m in the model and observed rainfall during November–December 2015 are shown. Comparison of Figs. 11a and 11b indicates that the model successfully captures the pattern of observed rainfall that led to the extreme flood event in Chennai during 2015. We explore the weather phenomenon that might have contributed to this extreme flood event. For this purpose, daily composites of rainfall and SLP for daily rainfall greater than 100 mm day^{-1} are shown for observation during November–December of 2015 and in the model.[2] The observed daily composite of SLP shows a low pressure over the Bay of Bengal, which is conducive for enhanced rainfall over Chennai (Figs. 12a,b). Composites of model-simulated daily rainfall and SLP also indicate extreme rainfall over Chennai, which is accompanied by favorable weather conditions such as low SLP near the coast over the Bay of Bengal (Figs. 12c,d). The only caveat in the model is that the SLP shows a deeper low and northward shift than observations. The differences between observations and the model may also be related to sampling variability, as the observational composite involves fewer days (3 days), whereas the model composite includes a large sample size (786 days). The relationship between Chennai rainfall and low pressure as seen in observations and the model is consistent with studies suggesting that extreme rainfall over Chennai is a result of persistent depression over the warm Bay of Bengal, which favors the transport of moisture from the Bay of Bengal (Narasimhan et al. 2016; Ray et al. 2016). The warm SSTs over the Bay of Bengal may

[2] Criterion of 100 mm day^{-1} is based on daily time series of rainfall shown in Ray et al. (2016), which indicates that the days with extreme rainfall over Chennai exceeded 100 mm day^{-1} during November –December of 2015.

TABLE 1. Probability of Bay of Bengal SSTs is listed in second row for criteria of Bay of Bengal SSTs shown in first row. Conditional probability of aggregate rainfall over Chennai greater than 1 m is listed in third row for the criteria of Bay of Bengal SSTs shown in first row.

	SST $< -2\sigma$	SST $< -1\sigma$	$-1\sigma >$ SST $< -2\sigma$	SST $> 1\sigma$	SST $> 2\sigma$
Probability (SST)	2.2%	16%	67%	16%	1.7%
Conditional probability ($P = 1$ m|SST)	0%	0.94%	1.7%	5.3%	8.8%

have also enhanced the possibility of occurrence of such low-pressure systems. We explore this possibility by analyzing the low SLP days during warm and cold Bay of Bengal events. Figure 13 suggests that warm Bay of Bengal SSTs tend to increase the number of days with low SLP relative to cold Bay of Bengal SSTs.

4. Conclusions and discussion

Chennai received an unprecedented amount of rainfall of 1416.8 mm during November–December of 2015, which caused immense loss of life and property. It is of utmost importance to understand if such events might occur in the future for planning and mitigation purposes. Thus, we investigate the probability of occurrence of such an extreme flood event over Chennai. We also explore the causes that might lead to such an intense event. Annual rainfall over Chennai is derived predominantly from the northeast monsoon. Previous studies highlight the role of SSTs in the Indian and Pacific Oceans in addition to global warming in the enhancement of the northeast monsoon. Thus, the main objective of this study is to determine the effect of ENSO, Indian Ocean SSTs, and radiative forcing in changing the odds of occurrence of extreme flood events over Chennai, similar to the one that was reported during November–December 2015.

Since there exists only a limited sample size in observations, to understand such rare extreme events, we make use of a suite of GFDL simulations to address our objective. We explored the ability of GFDL models, CM2.1, FLOR, FLOR-FA, and HiFLOR, to simulate the mean state, variability, and associated teleconnections of the northeast monsoon. FLOR and FLOR-FA have better simulation of the above-mentioned observed features of the northeast monsoon than CM2.1 and HiFLOR. Thus, we employ series of model simulations from FLOR and FLOR-FA to explore the probability of occurrence of Chennai-like extreme flood events in the future. For this purpose, we use the criterion of aggregate rainfall at Chennai (at a grid point: 13.08°N, 80.27°E) greater than 1 m to represent the Chennai flood event of 2015.

The probability of aggregate rainfall over Chennai greater than 1 m in a large 35-member ensemble run from FLOR-FA-20C3M shows an increasing trend after the 2000s, thus suggesting an increase in the odds of occurrence of Chennai-like flood events in future, which is consistent with observational studies (Rajeevan et al. 2012). However, a longer five-member ensemble run indicates that the trend after the 2000s is part of long-term variability. We also explore the probability of the

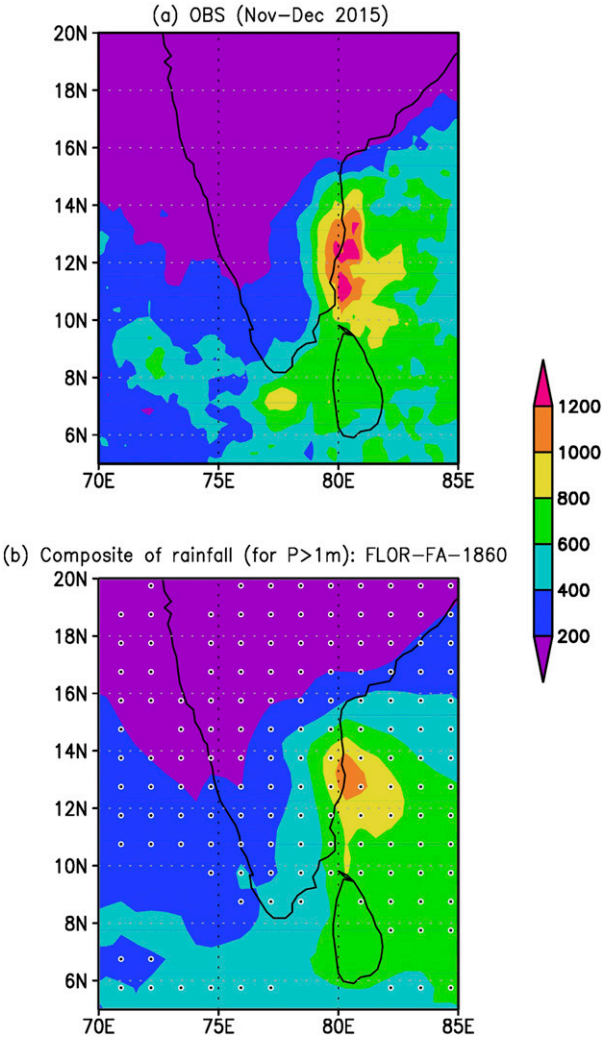

FIG. 11. (a) Obs rainfall during November –December of 2015 and (b) composite of rainfall for aggregate rainfall greater than 1 m for FLOR-FA-1860 during November –December. Units are in mm day^{-1}. Dotted regions represent values significant at 5% significance level.

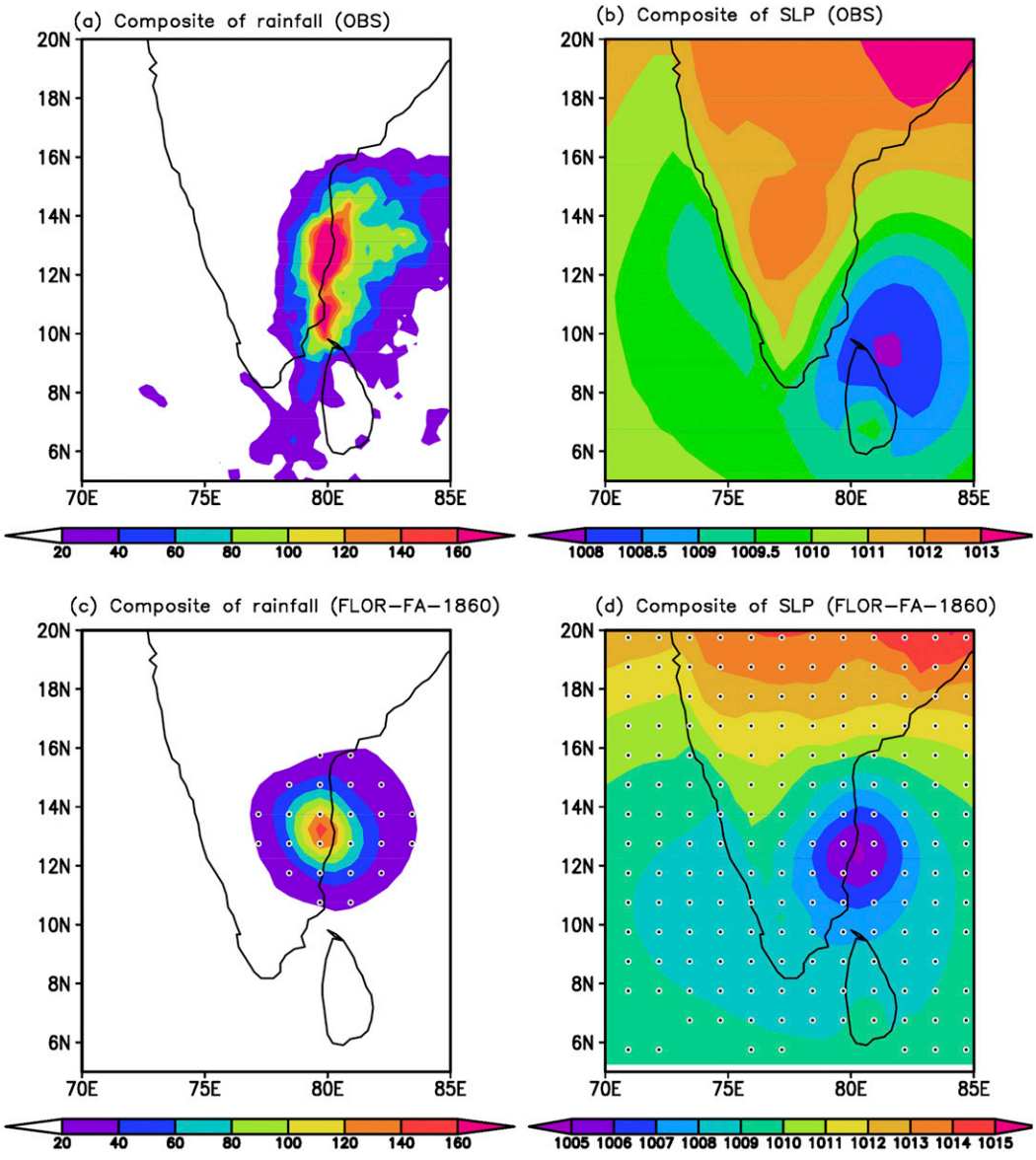

FIG. 12. Composite of (a) daily rainfall and (b) daily SLP during November –December of 2015 in observations, and (c) daily rainfall and (d) daily SLP based on daily rainfall greater than 100 mm day^{-1} in FLOR-FA-1860 during November –December. Units for rainfall and SLP are in mm day^{-1} and hPa. Dotted regions represent values significant at 5% significance level.

occurrence of Chennai-like flood events in a warming scenario by comparing the probability in double CO_2 runs to 1860 and 1990 control runs. Although the probability of extreme flood events increases from the 1860 to 1990 control run, the probability does not show a dramatic increase when greenhouse gas forcing is doubled. Therefore, there is no robust evidence indicating that the radiative forcing increases the odds of occurrence of extreme floods over Chennai. Van Oldenborgh et al. (2016) also concluded that extreme 1-day rainfall over Chennai does not show an increasing trend under global warming.

Several studies suggest that the large-scale SST forcing from the Indian and Pacific Oceans determines the variability of the northeast monsoon. Since a strong El Niño event coincided with the extreme flood event over Chennai during 2015, we determine the conditional probability of extreme flooding over Chennai during ENSO years. The probability of occurrence of intense flooding over Chennai is not sensitive to the state of the tropical Pacific, either to El Niño or La Niña. But the probability of occurrence of extreme floods over Chennai increases during the years when warm SSTs

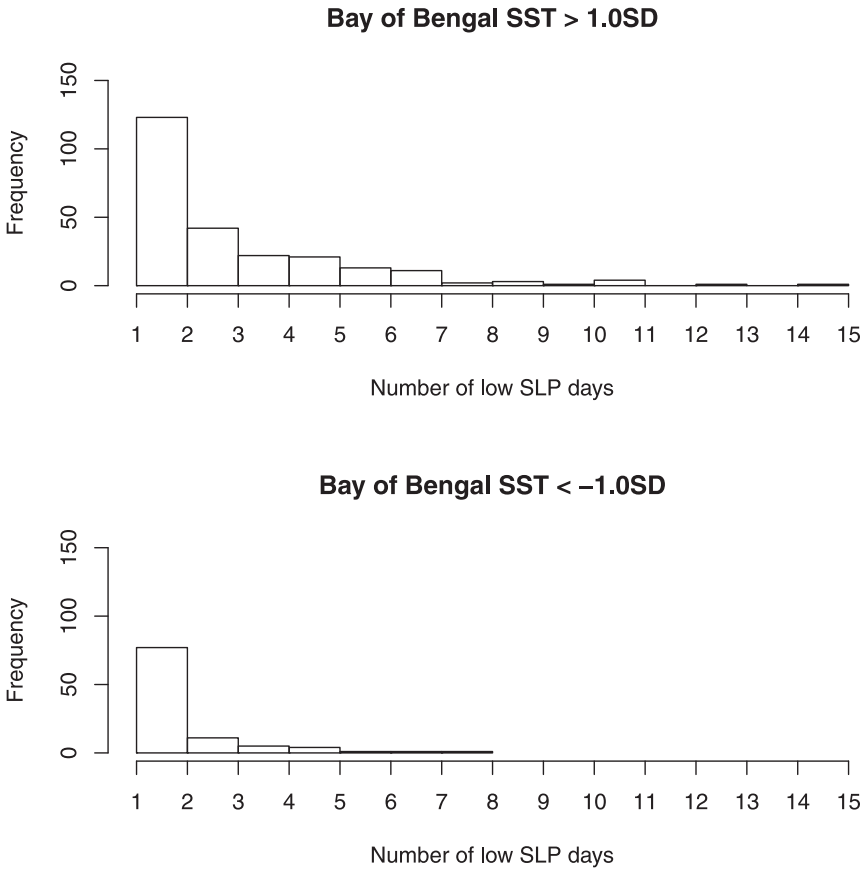

FIG. 13. Histogram of number of days SLP index is lower than 1007 hPa during years with the Bay of Bengal SST index (a) greater than 1.0 SD and (b) less than −1.0 SD in FLOR-FA-1860 during November–December. SLP index is defined as the area-averaged daily SLP over the domain [9°–15°N, 77°–83°E].

prevail over the Bay of Bengal. These results suggest that the local SSTs, rather than remote forcing, play a dominant role in changing the probability of floods over Chennai. The warm Bay of Bengal is known to induce more storms (Balaguru et al. 2014). In our analysis, composites of daily SLP in observations during 2015 and models indicate a low SLP over the Bay of Bengal collocated with warm Bay of Bengal SSTs, which favors the transport of moisture from warm oceanic regions to the land. We also show that the warm SSTs over the Bay of Bengal tend to increase the number of days with low SLP relative to cold SSTs. These atmospheric and oceanic conditions are conducive for an extreme flood event over Chennai. This is consistent with the results of Narasimhan et al. (2016), which indicate that the intense rainfall over Chennai was a result of enhanced moisture transported by a depression over the Bay of Bengal.

In this study, we reviewed extreme precipitation-induced flooding. Extreme precipitation alone does not lead to floods; land surface conditions and lack of proper storm management can play a significant role in causing or mitigating floods. It is suggested that the lack of proper urban infrastructure planning made the impacts of the Chennai flood worse (Jayaraman 2015); we hope the results of this study, which quantify the risk of Chennai precipitation extremes in the present and future climate, can help guide the planning of, for example, infrastructure and housing projects for future events. Thus, the results from this study that show that the years with warm Bay of Bengal SSTs may increase the odds of occurrence of a Chennai-like flood event are crucial for decision-makers for adaptation and mitigation purposes. This information will help them plan for any future risks that may be posed by extreme flooding over Chennai and in disaster preparedness and management. While this study provides insights on an individual event and its likelihood for change in the future, the methodologies and framework used in this investigation can be applied elsewhere.

Acknowledgments. Lakshmi Krishnamurthy is supported from Award NA14OAR4320106 from the National Oceanic and Atmospheric Administration,

U.S. Department of Commerce. The statements, findings, conclusions, and recommendations are those of the author(s) and do not necessarily reflect the views of the National Oceanic and Atmospheric Administration or the U.S. Department of Commerce. V. Balaji is supported by the Cooperative Institute for Climate Science, Princeton University, under Award NA08OAR4320752 from the National Oceanic and Atmospheric Administration. We thank Hiroyuki Murakami and Angel Munoz for helpful comments. We also thank three anonymous reviewers for their suggestions, which helped improve the manuscript. GPCP data is provided by the NOAA/OAR/ESRL PSD, Boulder, Colorado, USA, from their website at http://www.esrl.noaa.gov/psd/.

REFERENCES

Adler, R. F., and Coauthors, 2003: The version-2 Global Precipitation Climatology Project (GPCP) monthly precipitation analysis (1979–present). *J. Hydrometeor.*, **4**, 1147–1167, https://doi.org/10.1175/1525-7541(2003)004<1147:TVGPCP>2.0.CO;2.

Balaguru, K., S. Taraphdar, L. R. Leung, and G. R. Foltz, 2014: Increase in the intensity of postmonsoon Bay of Bengal tropical cyclones. *Geophys. Res. Lett.*, **41**, 3594–3601, https://doi.org/10.1002/2014GL060197.

Chen, S., R. Wu, W. Chen, B. Yu, and X. Cao, 2016: Genesis of westerly wind bursts over the equatorial western Pacific during the onset of the strong 2015–2016 El Niño. *Atmos. Sci. Lett.*, **17**, 384–391, https://doi.org/10.1002/asl.669.

Dee, D. P., and Coauthors, 2011: The ERA-Interim reanalysis: Configuration and performance of the data assimilation system. *Quart. J. Roy. Meteor. Soc.*, **137**, 553–597, https://doi.org/10.1002/qj.828.

Delworth, T. L., and F. Zeng, 2016: The impact of the North Atlantic Oscillation on climate through its influence on the Atlantic meridional overturning circulation. *J. Climate*, **29**, 941–962, https://doi.org/10.1175/JCLI-D-15-0396.1.

——, and Coauthors, 2012: Simulated climate and climate change in the GFDL CM2.5 high-resolution coupled climate model. *J. Climate*, **25**, 2755–2781, https://doi.org/10.1175/JCLI-D-11-00316.1.

DNA, 2015: Chennai flood losses estimated at Rs 20,034 crore to the India's economy, says Aon Benfield report. DNA, http://www.dnaindia.com/money/report-chennai-floods-losses-estimated-at-rs-20034-crore-to-the-india-s-economy-says-aon-benfield-report-2154521.

Jayaraman, N. 2015: Chennai floods are not a natural disaster—They've been created by unrestrained construction. Scroll, https://scroll.in/article/769928/chennai-floods-are-not-a-natural-disaster-theyve-been-created-by-unrestrained-construction.

Jia, L., and Coauthors, 2015: Improved seasonal prediction of temperature and precipitation over land in a high-resolution GFDL climate model. *J. Climate*, **28**, 2044–2062, https://doi.org/10.1175/JCLI-D-14-00112.1.

——, and Coauthors, 2016: The roles of radiative forcing, sea surface temperatures, and atmospheric and land initial conditions in U.S. summer warming episodes. *J. Climate*, **29**, 4121–4135, https://doi.org/10.1175/JCLI-D-15-0471.1.

Krishnamurthy, L., G. A. Vecchi, R. Msadek, A. Wittenberg, T. L. Delworth, and F. Zeng, 2015: The seasonality of the Great Plains low-level jet and ENSO relationship. *J. Climate*, **28**, 4525–4544, https://doi.org/10.1175/JCLI-D-14-00590.1.

——, ——, ——, H. Murakami, A. Wittenberg, and F. Zeng, 2016: Impact of strong ENSO on regional tropical cyclone activity in a high-resolution climate model in the North Pacific and North Atlantic Oceans. *J. Climate*, **29**, 2375–2394, https://doi.org/10.1175/JCLI-D-15-0468.1.

Kumar, P., K. Rupa Kumar, M. Rajeevan, and A. K. Sahai, 2007: On the recent strengthening of the relationship between ENSO and northeast monsoon rainfall over South Asia. *Climate Dyn.*, **28**, 649–660, https://doi.org/10.1007/s00382-006-0210-0.

Legates, D. R., and C. J. Willmott, 1990: Mean seasonal and spatial variability in gauge-corrected, global precipitation. *Int. J. Climatol.*, **10**, 111–127, https://doi.org/10.1002/joc.3370100202.

L'Heureux, M. L., and Coauthors, 2017: Observing and predicting the 2015/16 El Niño. *Bull. Amer. Meteor. Soc.*, **98**, 1363–1382, https://doi.org/10.1175/BAMS-D-16-0009.1.

Mishra, A. K., 2016: Monitoring Tamil Nadu flood of 2015 using satellite remote sensing. *Nat. Hazards*, **82**, 1431–1434, https://doi.org/10.1007/s11069-016-2249-5.

Msadek, R., K. W. Dixon, T. L. Delworth, and W. J. Hurlin, 2010: Assessing the predictability of the Atlantic meridional overturning circulation and associated fingerprints. *Geophys. Res. Lett.*, **37**, L19608, https://doi.org/10.1029/2010GL044517.

——, G. A. Vecchi, M. Winton, and R. G. Gudgel, 2014: Importance of initial conditions in seasonal predictions of Arctic sea ice extent. *Geophys. Res. Lett.*, **41**, 5208–5215, https://doi.org/10.1002/2014GL060799.

Murakami, H., and Coauthors, 2015a: Simulation and prediction of category 4 and 5 hurricanes in the high-resolution GFDL HiFLOR coupled climate model. *J. Climate*, **28**, 9058–9079, https://doi.org/10.1175/JCLI-D-15-0216.1.

——, G. A. Vecchi, T. L. Delworth, K. Paffendorf, R. Gudgel, L. Jia, and F. Zeng, 2015b: Investigating the influence of anthropogenic forcing and natural variability on the 2014 Hawaiian hurricane season [in "Explaining Extreme Events of 2014 from a Climate Perspective"]. *Bull. Amer. Meteor. Soc.*, **96** (12), S115–S119, https://doi.org/10.1175/BAMS-D-15-00119.1.

Naidu, C. V., G. C. Satyanarayana, K. Durgalakshmi, L. M. Rao, G. J. Mounika, A. D. Raju, 2012: Changes in the frequencies of northeast monsoon rainy days in the global warming. *Global Planet. Change*, **92–93**, 40–47, https://doi.org/10.1016/j.gloplacha.2012.04.009.

Narasimhan, B., S. M. Bhallamudi. A. Mondal. S. Ghosh, and P. Mujumdar, 2016: Chennai floods 2015: A rapid assessment. Interdisciplinary Centre for Water Research Rep., 43 pp.

Nayagam, L. R., R. Janardanan, and H. S. Ram Mohan, 2009: Variability and teleconnectivity of northeast monsoon rainfall over India. *Global Planet. Change*, **69**, 225–231, https://doi.org/10.1016/j.gloplacha.2009.10.005.

Pascale, S., S. Bordoni, S. B. Kapnick, G. A. Vecchi, L. Jia, T. L. Delworth, S. Underwood, and W. Anderson, 2016: The impact of horizontal resolution on North American monsoon Gulf of California moisture surges in a suite of coupled global climate models. *J. Climate*, **29**, 7911–7936, https://doi.org/10.1175/JCLI-D-16-0199.1.

Prakash, S., C. Mahesh, V. Sathiyamoorthy, and R. M. Gairola, 2013: Increasing trend of northeast monsoon rainfall over the equatorial Indian Ocean and peninsular India. *Theor. Appl. Climatol.*, **112**, 185–191, https://doi.org/10.1007/s00704-012-0719-6.

Rajeevan, M., C. K. Unnikrishnan, J. Bhate, K. Niranjan Kumar, and P. P. Sreekala, 2012: Northeast monsoon over India:

Variability and prediction. *Meteor. Appl.*, **19**, 226–236, https://doi.org/10.1002/met.1322.

Ray, K., B. A. M. Kannan, S. Stella, B. Sen, P. Sharma, and S. B. Thampi, 2016: Heavy rains over Chennai and surrounding areas as captured by Doppler weather radar during northeast monsoon 2015: A case study. *Remote Sensing of the Atmosphere, Clouds, and Precipitation VI*, E. Im, R. Kumar, and S. Yang, Eds., International Society for Optics and Photonics (SPIE Proceedings, Vol. 9876), 98762G, https://doi.org/10.1117/12.2239563.

Rayner, N. A., D. E. Parker, E. B. Horton, C. K. Folland, L. V. Alexander, D. P. Rowell, E. C. Kent, and A. Kaplan, 2003: Global analyses of sea surface temperature, sea ice, and night marine air temperature since the late nineteenth century. *J. Geophys. Res.*, **108**, 4407, https://doi.org/10.1029/2002JD002670.

Selvaraj, K., J. Pandiyan, V. Yoganandan, and G. Agoramoorthy, 2016: India contemplates climate change concerns after floods ravaged the coastal city of Chennai. *Ocean Coastal Manage.*, **129**, 10–14, https://doi.org/10.1016/j.ocecoaman.2016.04.017.

Simpson, J., C. Kummerow, W.-K. Tao, and R. F. Adler, 1996: On the Tropical Rainfall Measuring Mission (TRMM). *Meteor. Atmos. Phys.*, **60**, 19–36, https://doi.org/10.1007/BF01029783.

van der Wiel, K., and Coauthors, 2016: The resolution dependence of contiguous U.S. precipitation extremes in response to CO_2 forcing. *J. Climate*, **29**, 7991–8012, https://doi.org/10.1175/JCLI-D-16-0307.1.

——, and Coauthors, 2017: Rapid attribution of the August 2016 flood-inducing extreme precipitation in south Louisiana to climate change. *Hydrol. Earth Syst. Sci.*, **21**, 897–921, https://doi.org/10.5194/hess-21-897-2017.

van Oldenborgh, G. J., F. E. L. Otto, K. Haustein, and K. AchutaRao, 2016: The heavy precipitation event of December 2015 in Chennai, India [in "Explaining Extreme Events of 2015 from a Climate Perspective"]. *Bull. Amer. Meteor. Soc.*, **97** (12), S87–S91, https://doi.org/10.1175/BAMS-D-16-0129.1.

Vecchi, G. A., and B. J. Soden, 2007: Effect of remote sea surface temperature change on tropical cyclone potential intensity. *Nature*, **450**, 1066–1070, https://doi.org/10.1038/nature06423.

——, and Coauthors, 2014: On the seasonal forecasting of regional tropical cyclone activity. *J. Climate*, **27**, 7994–8016, https://doi.org/10.1175/JCLI-D-14-00158.1.

Winton, M., W. G. Anderson, T. L. Delworth, S. M. Griffies, W. J. Hurlin, and A. Rosati, 2014: Has coarse ocean resolution biased simulations of transient climate sensitivity? *Geophys. Res. Lett.*, **41**, 8522–8529, https://doi.org/10.1002/2014GL061523.

Xie, S.-P., C. Deser, G. A. Vecchi, J. Ma, H. Teng, and A. T. Wittenberg, 2010: Global warming pattern formation: Sea surface temperature and rainfall. *J. Climate*, **23**, 966–986, https://doi.org/10.1175/2009JCLI3329.1.

Yadav, R. K., 2012: Why is ENSO influencing Indian northeast monsoon in the recent decades? *Int. J. Climatol.*, **32**, 2163–2180, https://doi.org/10.1002/joc.2430.

——, 2013: Emerging role of Indian Ocean on Indian northeast monsoon. *Climate Dyn.*, **41**, 105–116, https://doi.org/10.1007/s00382-012-1637-0.

Yang, X., G. A. Vecchi, T. L. Delworth, K. Paffendorf, L. Jia, R. Gudgel, F. Zeng, and S. D. Underwood, 2015: Extreme North America winter storm season of 2013/14: Roles of radiative forcing and the global warming hiatus [in "Explaining Extreme Events of 2014 from a Climate Perspective"]. *Bull. Amer. Meteor. Soc.*, **96** (12), S25–S28, https://doi.org/10.1175/BAMS-D-15-00133.1.

Yatagai, A., K. Kamiguchi, O. Arakawa, A. Hamada, N. Yasutomi, and A. Kitoh, 2012: APHRODITE: Constructing a long-term daily gridded precipitation dataset for Asia based on a dense network of rain gauges. *Bull. Amer. Meteor. Soc.*, **93**, 1401–1415, https://doi.org/10.1175/BAMS-D-11-00122.1.

Zhang, L., and T. L. Delworth, 2015: Analysis of the characteristics and mechanisms of the Pacific decadal oscillation in a suite of coupled models from the Geophysical Fluid Dynamics Laboratory. *J. Climate*, **28**, 7678–7701, https://doi.org/10.1175/JCLI-D-14-00647.1.

Zhang, W., and Coauthors, 2016: Influences of natural variability and anthropogenic forcing on the extreme 2015 accumulated cyclone energy in the western North Pacific [in "Explaining Extreme Events of 2015 from a Climate Perspective"]. *Bull. Amer. Meteor. Soc.*, **97** (12), S131–S135, https://doi.org/10.1175/BAMS-D-16-0146.1.

Zubair, L., and C. F. Ropelewski, 2006: The strengthening relationship between ENSO and northeast monsoon rainfall over Sri Lanka and southern India. *J. Climate*, **19**, 1567–1575, https://doi.org/10.1175/JCLI3670.1.